coatings

Review

Progress on the Properties of Ceramic Phase-Reinforced High-Entropy Alloy Composite Coatings Produced via Laser Cladding

Haoran Zhang [1,2,3], Yaowei Yong [2,*], Fuwei Wang [1,3], Yuan Liang [1,3], Lin Liu [4], Hong Liu [1,3] and Yang Gao [1,3,*]

[1] College of Mechatronic Engineering, North Minzu University, Yinchuan 750021, China; 18738712334@163.com (H.Z.); wang_fuwei@nmu.edu.cn (F.W.); ly18895087502@163.com (Y.L.); hlongiu@163.com (H.L.)
[2] School of Mechanical Engineering, Ningxia University, Yinchuan 750021, China
[3] Ningxia Engineering Research Center for Hybrid Manufacturing System, Yinchuan 750021, China
[4] Department of Mechanical Engineering, University of Kansas, Lawrence, KS 66045, USA; linliu@ku.edu
* Correspondence: yywnxu@163.com (Y.Y.); 2008034@nmu.edu.cn (Y.G.)

Abstract: The production of ceramic phase-reinforced high-entropy alloy composite coatings with excellent mechanical properties, high-temperature oxidation resistance, and corrosion resistance via laser cladding is a new hotspot in the field of surface engineering. However, as high-entropy alloys have a wide range of constituent systems and different kinds of ceramic particles are introduced in different ways that give the coatings unique microscopic organization, structure, and synthesized performance, it is necessary to review the methods of preparing ceramic phase-reinforced high-entropy alloys composite coatings via laser cladding. In this paper, the latest research progress on laser cladding technology in the preparation of ceramic phase-reinforced high-entropy alloy composite coatings is first reviewed. On this basis, the effects of ceramic particles, alloying elements, process parameters, and the microstructure and properties of the coatings are analyzed with the examples of the in situ generation method and the externally added method. Finally, research gaps and future trends are pointed out, serving as a reference for the subsequent research, application, and development of the preparation of ceramic phase-reinforced high-entropy alloy composite coatings.

Keywords: laser cladding; surface modification; ceramic reinforcement; protective coatings; high-entropy alloy; fabrication methods

Citation: Zhang, H.; Yong, Y.; Wang, F.; Liang, Y.; Liu, L.; Liu, H.; Gao, Y. Progress on the Properties of Ceramic Phase-Reinforced High-Entropy Alloy Composite Coatings Produced via Laser Cladding. *Coatings* **2024**, *14*, 127. https://doi.org/10.3390/coatings14010127

Academic Editor: Avik Samanta

Received: 18 December 2023
Revised: 12 January 2024
Accepted: 16 January 2024
Published: 18 January 2024

1. Introduction

High-entropy alloys (HEAs) are a category of alloys constituted by five or more elemental components combined in equiatomic or near-equiatomic proportions. These alloys are characterized by a mixing entropy that exceeds the melting entropy of the alloy, enabling the formation of a high-entropy solid-solution phase [1]. High-entropy alloys, also known as multiprincipal element alloys, were discovered in 2004 by Ye et al. [2] from Taiwan, and Cantor et al. [3] from Brition published the research results of preparing HEAs; since then, a research upsurge of HEAs was set off. High-entropy alloys have four main effects: a high entropy effect in thermodynamics, a lattice distortion effect in structure, a hysteresis diffusion effect in dynamics, and a cocktail effect in properties [4,5]. These four effects allow it to exhibit many excellent properties that are superior to traditional alloys, such as high fatigue resistance [6], hardness [5], high wear resistance [7], excellent corrosion resistance [8], and good thermal stability [9]. Bulk amorphous alloys have become a new research area and represent an important direction of the future development of materials. Because of the highly mixed entropies of these alloys, they form solid solutions with simple crystalline structures in which CoCrCuFeNi acts as a representative of a face-centered cubic solid solution (FCC), body-centered cubic solid solution (BCC) supported by AlCoCrFeNi, and hexagonal close packing (HPC). The orthorhombic structure or a combination of these phases can be achieved by altering the high-entropy alloying elements. The combination of high-entropy alloy coatings and new surface treatment technologies provides new research ideas to enhance the comprehensive performance of the base material, such as hardness, wear resistance, and corrosion resistance. In the last decade, researchers have been investigating the mechanisms of laser-cladded coatings to improve the overall performance of coatings for industrial applications. Studies have indicated that adding ceramic particles to high-entropy alloys can significantly improve the mechanical properties of coatings, wear resistance, and other comprehensive properties [10,11]. Ceramic particles have superior properties, such as high-temperature resistance and wear resistance. Usually, the addition of ceramic particles in composites can significantly improve the hardness and wear resistance of the composites so as to obtain composites with excellent performance. Liu et al. [12] added solid lubricant (MoS_2) and hard ceramic-reinforcing particles (B_4C) in an Al 7075 aluminum alloy matrix alloy, which is used for automotive hybrid aluminum composites so that the abrasion resistance and the coefficient of friction of aluminum hybrid composites can be significantly improved. Ceramic particles are often introduced into high-entropy alloys (Figure 1), which are mainly divided into metal ceramics and non-metal ceramics and their selection, which is based on suitable ceramic content and the matching between ceramics and high entropy. Selecting the appropriate ceramic content and matching ceramic and high-entropy alloy coatings is the key to ensuring the strong synergistic performance of the molten cladding layer. High-entropy alloy composite coating materials integrate the superior strength, toughness, and processability of metals with the outstanding wear resistance and corrosion resistance of ceramics, thus amalgamating the merits of both material categories, expanding the prospects for combining materials science and metallurgy, and providing a potential new research direction for the manufacture of materials with high abrasion resistance, corrosion resistance, and other high-end needs [13,14].

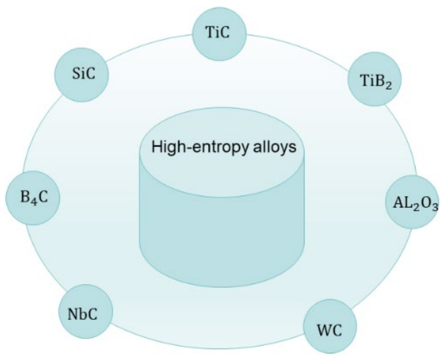

Figure 1. Types of ceramic particles often involved in high-entropy alloys.

The manufacturing processes for high-entropy alloy coatings include a variety of main processes, including magnetron sputtering [15], laser cladding [16], electrodeposition [17], plasma spraying [18], etc. Laser cladding is the preparation of a selected powder system on the surface of the substrate. It uses a high-energy density laser as a heat source to melt the material on the surface of the workpiece substrate, form a coating with special physicochemical properties, and achieve the connection of the coating. The substrate material is a large amount of protective gas required to prevent oxidation of the melting process during the laser cladding process. Ultrasound assistance and monitoring systems are usually added. The laser coating equipment and the heat-affected zone of the coating process are illustrated in Figure 2. To date, laser cladding and thermal spraying are the more popular methods to prepare high-entropy alloy coatings. The combination of thermal spraying coating and the substrate is mainly mechanical inlay, while the combination of laser cladding coating and the substrate is a metallurgical combination, which has better performance under heavy load impact. Mu et al. [19] used thermal spraying technology to prepare AlCoCrFeNi high-entropy alloy coatings compared with Cai et al. [20], who used the laser cladding method to prepare FeCoCrNiAl; it can be clearly seen that the laser cladding method of high-entropy alloy coatings has the characteristics of small deformation, high density, low dilution, a wide range of powder selection, good metallurgical bonding, etc. It is obvious that the high-entropy alloy coatings prepared via laser cladding have the characteristics of small deformation, high density, low dilution rate, a wide range of powder selection, and good metallurgical bonding [21,22]. In the current manufacturing field, the production of high-performance coatings via laser deposition welding is a key solution for achieving complex, extreme, highly sensitive, and efficient application environments, which offers wide developmental potential in repairing defective parts and improving the mechanical properties of workpiece surfaces and is usually applied in the fields of aerospace, machinery, and medical equipment [23,24].

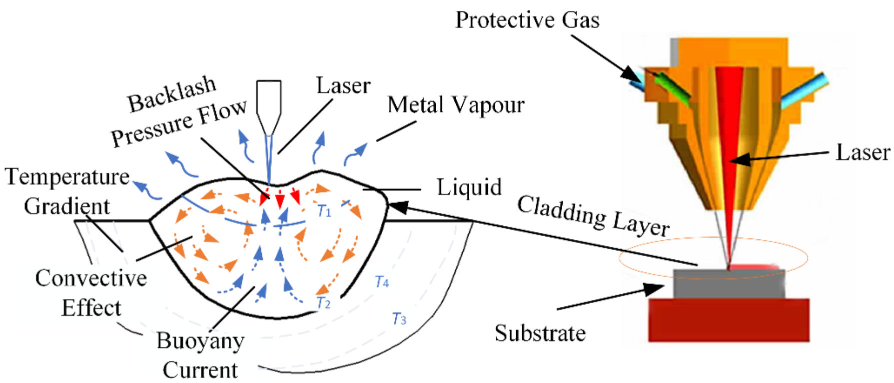

Figure 2. Heat-affected zone (HAZ) with melt pool and device schematic.

The frictional wear of mechanical components during operation leads to a shortening of the service life of components and the failure of machinery and equipment, resulting in a large waste of energy and materials. More than 30% of the world's available energy is lost due to friction and wear, and more than 70% of industrial components are scrapped due to friction and wear [25]. In aviation, navigation, and related fields, materials are subjected to stringent demands for corrosion resistance, high-temperature wear resistance, and oxidation resistance. For example, 304 stainless steels are popularly utilized in vehicles, marine, and other fields, which have superior corrosion prevention and mechanical properties but poor hardness and wear resistance. TC4 alloy is usually applied in the aerospace field, with higher requirements for hardness and wear properties. The use of high-entropy alloy composite coatings reinforced with a ceramic phase on the surface of critical parts is therefore considered to be an effective way to enhance the comprehensive performance of the parts. Therefore, numerous researchers have used surface modification techniques such as CMT to increase mechanical properties such as wear resistance and hardness of mechanical parts [26]. The preparation of ceramic phase-reinforced high-entropy alloy composite coatings on the surface of critical parts is an effective method to enhance the comprehensive performance of the parts. Laser coating preparation is used for ceramic phase-reinforced high-entropy alloy composite coatings with excellent corrosion resistance, wear resistance, and high hardness. Most researchers focus on the alloying element ratio of the high-entropy alloy coating, the parameters of the coating process, and the heat treatment process on the coating properties of the research. The production method of high-entropy alloy composite coatings and the correlation between the microstructure and the performance of the high-entropy alloy composite coatings summarized are still insufficient. The present paper reviews the research progress of ceramic phase-reinforced high-entropy alloy composite coatings in recent years. It focuses on the analysis and summary of the method of producing composite coatings in terms of the microstructure and properties of high-entropy alloy composite coatings. The purpose of this analysis is for the future use of laser cladding for the production of composite coatings from high-entropic alloys and to conduct in-depth research to bring enlightenment.

2. Preparation of Ceramic Phase-Reinforced High-Entropic Alloy Composite Coatings

Different composition systems of high-entropic alloys determine the clad layer's mechanical, physical, and electrochemical properties and the workpiece's application range after cladding. The production of high-entropy alloy composite coatings on the surface of the substrate using laser cladding is divided into two main categories: the in situ generation method and the additive method, as depicted in Figure 3. Using the above two methods, the high-entropy alloy composite coating used to introduce the ceramic phase can be caused by the transformation of the internal phase structure of the coating. Changes in grain size or the formation of new phases contribute to enhancements in the hardness, wear resistance, corrosion resistance, high-temperature oxidation resistance, and other properties of the high-entropy composite coating.

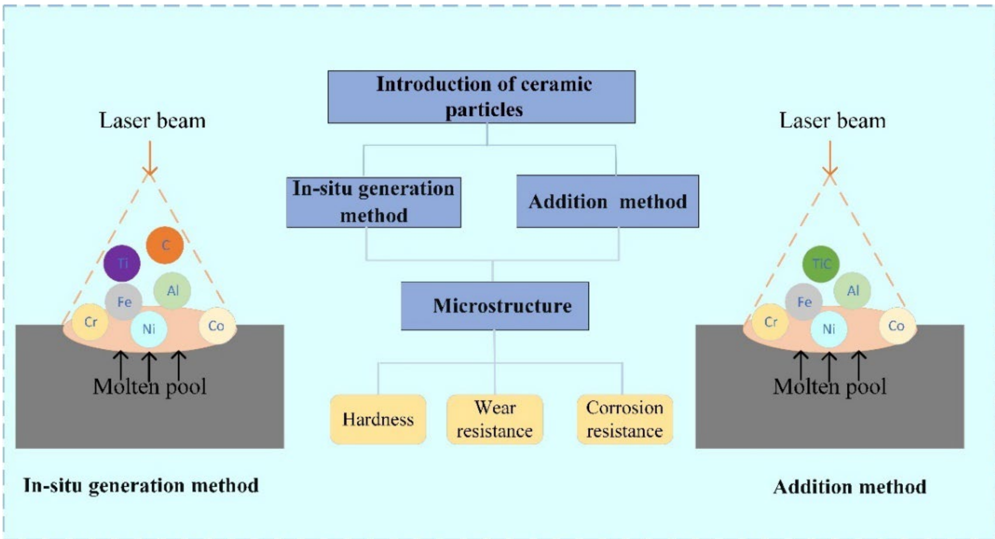

Figure 3. Schematic diagram of the introduction method of ceramic particles.

2.1. In Situ Generation Method

The in situ generation method refers to the in situ generation of the ceramic phase during the preparation of composite coatings and is based on the reaction between the raw materials or between the raw materials and the surrounding gases in the plasma. It is based on the original method of the in situ generation of metal/ceramic composite coatings, high-entropic alloy as a metal base, in situ generation of ceramic phase to improve the mechanics of high-entropic alloy composite coatings, and other comprehensive achievements. Preparing in situ-generated ceramic phase high-entropy alloy-based composite coatings using laser cladding is an effective method to solve the problem of poor interfacial bonding between ceramic particles and the metal matrix [27]. This method prepares the composite coatings with a simple process and a high deposition rate, and the matrix and composite ceramic phase possess good bonding properties and wettability. The ceramic particles generated in situ by the chemical reaction are disposed uniformly in the metal matrix, which reduces the influence between the interfaces and improves the overall performance and service life of the coating. Some researchers, including Feng et al. [28], Yang et al. [29], and Lin et al. [30], used the in situ generation of ceramic particles such as borides and carbides to significantly elevate the properties of entropy alloy coatings in terms of hardness, wear resistance, and corrosion resistance.

Guo et al. [31] successfully fabricated in situ-generated TiC ceramic-reinforced CoCr CuFeNiSi$_{0.2}$ coatings on 304 stainless steel via laser cladding. The experimental results show that with the increase of Ti and C, the composite coating CoCrCuFeNiSi$_{0.2}$ (Ti, C)$_x$ change from a single FCC solid-solution structure to an FCC Solid-solution structure. With the addition of Ti and C, the in situ TiC ceramics are mainly distributed at the grain boundaries. It can be observed that the coating has a typical dendritic structure at (Ti, C)$_0$, and as the (Ti, C)$_x$ content increases, white particles gradually appear in the grain boundaries, and the size of the white particles gradually increases. The white particles are in situ-generated TiC particles. The in situ-generated TiC particles perform solid-solution strengthening and diffusion strengthening on the high-entropy coating, which significantly increases the hardness and wear resistance of the coating. With a maximum hardness of 517.2 $HV_{0.2}$ and an average microhardness of 498.5 $HV_{0.2}$, the (Ti, C)$_{1.0}$ coating has the highest hardness, nearly 2 points higher than the HEA coatings without Ti and C. The hardness of the (Ti, C)$_{1.5}$ coating is lower than that of the (Ti, C)$_{1.0}$ coating, but as the content of Ti and C increases, the size of the TiC particles generated in situ in the coating increases as well, weakening the reinforcing effect. (Ti, C)$_{1.0}$ has the best wear performance; the gradual increase in TiC ceramic produced in situ lowers the coefficient of friction of the $CoCrCuFeNiSi_{0.2}$HEA coatings and significantly improves the coating's resistance to abrasion. During the wear process, (Ti, C)$_{1.5}$ large ceramic particles exert a plowing effect on the coating, making wear grooves on the surface more noticeable.

The performance of high-entropic alloy composite coatings is strongly influenced by the size of in situ-generated ceramic particles. Liu et al. [32] produced AlCoCrFeNiTix reinforced with TiC particles in situ that were authigenic using laser cladding on the surface of AISI 1045 steel. In contrast to that, Guo et al. [31] used the laser thinning effect to extract the high-entropic Fe and C elements in the coatings from the AISI 1045 steel matrix. Two BCC phases, Fe-Cr and Al-Ni, along with a trace amount of in situ TiC phase in the form of micro- and nanoparticle-sized particles, made up the coatings. The composite coatings of $CoCrCuFeNiTi_{1.0}$ HEA with the highest average microhardness (860.1 $HV_{0.3}$) exhibited a direct correlation with the increased volume fraction of the TiC particle phase (2.6%). The three-dimensional morphological characteristics and height analysis curves of the wear of the CTi_0 coating and the $CTi_{1.0}$ coating at high-temperature conditions are provided. The wear mechanism of this coating at high-temperature coating is mainly oxidative and adhesive wear. Compared with the wear characteristics under ambient conditions, the wear under high-temperature conditions exhibits bumps caused by plastic deformation rather than obvious furrows. According to the results of the height analysis, the height variation in the wear region of the $CTi_{1.0}$ coating is significantly smaller than that of the CTi_0 coating. These results suggest the existence of oxidative wear during the wear process, especially at high temperatures, which is usually associated with frictional heat. The micro- and nano-sized TiC particles improve the coating hardness and high-temperature friction resistance via solid-solution strengthening, diffusion strengthening, and grain refinement, demonstrating that oxidative and adhesive wear are the primary mechanisms of the coating's wear at high temperatures. Compared to high-entropy alloy coatings, different ceramics have different mechanisms and reinforcing effects. Zhou et al. [33] examined the effects of two ceramic particles, B_4C and SiC, on the mechanical properties and microstructure of CoCrMoNbTi high-entropy alloy coatings. The findings indicated that B_4C had the strongest strengthening effect on the high-entropy alloy coating's properties. The coating's microhardness increased from 666.2 $HV_{0.5}$ to 886.9 $HV_{0.5}$, which was attributed to the in situ generation of TiC during the melting process from C and Ti elements in the TC_4 substrate, which served as a role in precipitation reinforcement and grain refining on the coating. Additionally, the alloy's room temperature abrasion resistance was improved, and the coefficient of friction and wear rate were significantly decreased.

Refractory alloying components (e.g., G., Nb, Ta, W, Mo, and V) cause HEA coatings to exhibit lattice distortion, obstruct dislocation motion, and encourage the development of BCC phases, thereby fortifying the coatings with the solid solution. Additionally, their larger atomic radius typically results in an increase in the solid solution's lattice constant [34], enhancing the coatings' mechanical qualities and wear resistance. Recent studies by Chang et al. [35], Xiang et al. [36], Liu et al. [37], and Li et al. [38] examined the effects of refractory alloying elements on the characteristics of high-entropy alloy coatings. Based on how well strength, plasticity, and density match, refractory alloy elements can be broadly categorized into three groups. The first group is made up of high-density W and Mo alloys as well as other elements from the fifth and sixth subgroups. The second group is made up of low-density, high-plasticity, and high-entropy refractory alloys that contain elements from the fourth subgroup with lower density, like B, Ti, Zr, and Hf. The third category consists of elements from the third period that are added to the previously listed elements, like Al and Si. The third category combines refractory alloys with high entropy, modified strength, and toughness with third-cycle elements like Al and Si. The coordinated action of ceramic phases and refractory alloy elements is studied in high-entropy alloy composite coatings to generate new research ideas for coatings with high abrasion resistance and excellent mechanical properties. In their study, Zhao et al. [39] investigated the synergistic effect of Mo and in situ TiC on AlCoCrFeNi HEA coatings. They found that the grain size of the coating was only 1/24 of that of the AlCoCrFeNi coatings. Additionally, the hardness of the coating increased by 69.3%, and the wear resistance improved by 5.77 times due to the synergistic effect of Mo and in situ TiC.

TiB and TiC are ceramic-reinforced particles known for their excellent performance. TiB exhibits exceptional physical and thermomechanical properties [40], boasting a remarkable hardness of up to 27 GPa. On the other hand, TiC possesses a high modulus of elasticity, high hardness, low coefficient of friction, excellent chemical stability, and good wettability with the metal substrate. Additionally, coatings containing an excess of elemental Ti in solid-solution form not only significantly enhance the base material's mechanical properties and wear resistance [41] but also act as a solid lubricant, thereby reducing the coating wear rate. These properties make it a promising candidate for improving high-entropy alloy coatings. However, the in situ generation of single TiB_2 ceramic particles for high-entropy alloy coatings exhibits poor high-temperature oxidation properties and low fracture toughness. To overcome these limitations, incorporating two or more ceramic-reinforcing phases has been explored to enhance the thermal stability of high-entropy alloy coatings and achieve coating grain refinement. The resulting high-entropy alloy composite coatings exhibit high hardness, high wear resistance, and high-temperature oxidation resistance [42–44]. He et al. [45] conducted a study on the preparation of CoCrMoNbTi high-entropy alloy coatings by adding B_4C on a titanium alloy substrate using a laser melting technique. The researchers observed that as the B_4C content increased, the solid phase in the coating underwent three stages: $BCC_1 + BCC_2 \rightarrow BCC_1 + BCC_2 + TiC \rightarrow BCC_1 + BCC_2 + TiC + TiB$. In addition, two ceramic-reinforced phases, TiC and TiB, were generated in situ. These ceramic particles were found to be diffusely distributed in the coating and exhibited different morphologies. The presence of these particles inhibited grain growth and resulted in grain refinement, leading to a submicron grain size. The hardness of the coating increased from 666.26 $HV_{0.5}$ to 954.11 $HV_{0.5}$, and Young's modulus increased from 168.88 GPa to 240.35 GPa. These enhancements significantly improved the hardness and tensile strength of the coating. Yan et al. [46] successfully prepared in situ Ti (C, N)-reinforced AlCoCrFeNiSi high-entropy alloy coatings with a functional gradient bilayer structure on an H13 steel substrate. This study aimed to address the poor toughness and brittleness issues of the coatings. Unlike previous studies by He et al. [45] and others, Yan et al. [46] utilized Ti and C powders as precursor reactants for Ti (C, N) ceramic particles and high-purity nitrogen as the protective gas. The involvement of nitrogen in the coating reaction resulted in the in situ generation of Ti (C, N) ceramic particles. The microhardness of the coatings and the results of the EBSD and EDS analyses are depicted in Figures 4 and 5. This study indicates that the coatings prepared via this method possess a double gradient. The first layer is an FCC solid solution, and the second layer is a mixture of disordered BCC phase (Fe-Cr) and ordered B_2 phase (Al-Ni-Ti). It has a high content of Ti (C, N) ceramic particles and $TiSi_2$ speckled between grain boundaries in the microstructure. The high hardness of the second layer is attributed to the diffuse reinforcement induced by the ceramic particles. The in situ-generated Ti (C, N) ceramic particles, as non-deformable particles, effectively enhance the surface hardness of the HEA gradient coating. Additionally, the reticular $TiSi_2$ distribution along the body-centered cubic grain boundaries impedes grain boundary migration and contributes to the microstructure refinement, further enhancing the high hardness of the second layer. The main wear mechanisms of the coating are oxidative wear and a small amount of abrasive wear. The strong interfacial bonding between the in situ-generated Ti (C, N) particles and the HEA substrate provides the coating with high surface hardness and resistance to plastic deformation. Similar to Yan et al., Liu et al. [47] utilized high-purity nitrogen as a protective gas to melt-coat FeCoNiCrMnTix (atomic ratio x = 0, 0.5, 1.0, and 1.5) HEA-coated high-entropy alloy coatings onto the surface of 304 stainless steel in order to produce high-quality, defect-free coatings. This process resulted in the in situ formation of TiN particles. The coating is composed of the FCC phase, TiN phase, and Laves phase. As the Ti content (x = 0, 0.5, 1.0, and 1.5) increases, a stepped crystalline morphology gradually forms, and the amount of TiN particles in the coating increases, thereby enhancing the wear resistance of the coating. However, when the Ti content exceeds 1.0 reduced defects in coatings.

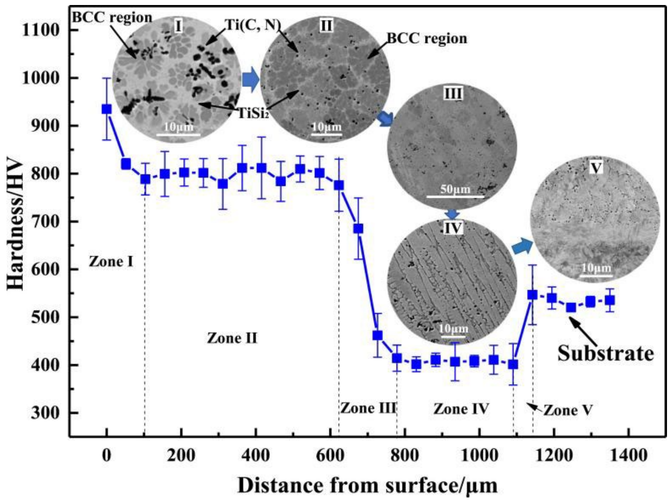

Figure 4. The hardness profile and corresponding microstructures of the HEA gradient coating [46].

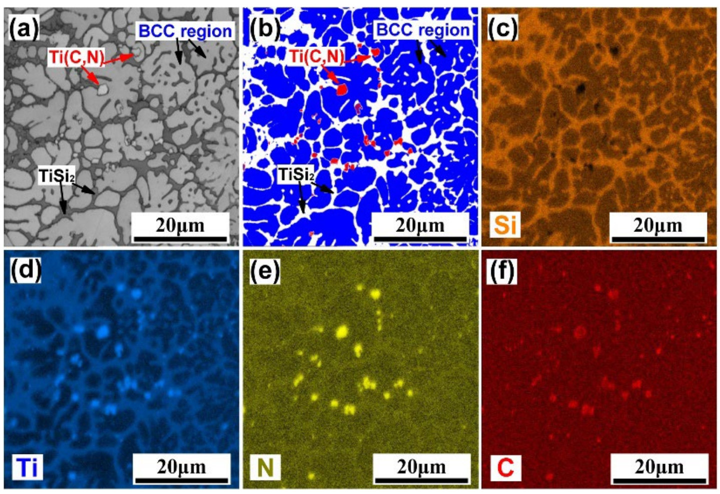

Figure 5. The EBSD and EDS results of microstructures in zone I: (**a**) EBSD band contrast (BC) map, (**b**) EBSD phase map, (**c**–**f**) EDS element distribution maps for Si, Ti, N, and C [46].

Currently, laser cladding primarily utilizes various in situ generation methods to enhance the ceramic phase. These methods include in situ single generation, in situ single generation with high melting point element doping, in situ double generation, in situ multi-gradient generation, and others. These methods are illustrated in Figure 6. Research has shown that ceramic particles generated in situ from some elements in the matrix are concentrated in the submicron or micro-nanometer level and exhibit uniform distribution.

Increasing the ceramic particle content effectively enhances the composite coating's hardness, wear resistance, and high-temperature abrasion resistance. However, the overall content of ceramic particles in the composite coatings is relatively low. Alternatively, content generated in situ are added to the elements to obtain a relatively high ceramic content in the entropy alloy composite coatings. In that case, the size of the ceramic particles will gradually increase with the increase in element content. Once the ceramic particles reach a certain size, the comprehensive performance of the composite coatings will decrease. Therefore, it is necessary to investigate the optimal content ratio of the elements to obtain excellent performance of the coatings when using this method to obtain ceramic particles. The in situ generation of single-phase ceramic phases is a straightforward process, allowing for the easy prediction and analysis of the phase composition of the composite coating after fusion coating. The combined action of high melting point elements and ceramic phases can further refine the grains and enhance composite coatings' wear resistance and mechanical properties compared to the generation of single ceramic phases. However, the high melting point elements come at a higher cost. The in situ generation of dual ceramic phases compensates for the single ceramic phase's limitations in terms of high-temperature oxidation and other properties. Building on this, in situ multi-ceramic phase gradient generation solves the issue of poor toughness in the coating. It can yield composite coatings with good hardness and plastic properties by increasing the ceramic content. Nevertheless, the method of coating preparation becomes more complex, and controlling the composition of the coating phase in each layer and the overall ceramic content is challenging. Each method has its advantages and disadvantages. However, different in situ generation methods can yield different phases and unique microstructures, further enhancing the hardness, abrasion resistance, high-temperature oxidation resistance, and corrosion resistance of high-entropy alloy coatings. These methods provide new design ideas for obtaining high-quality, high-entropy alloy coatings.

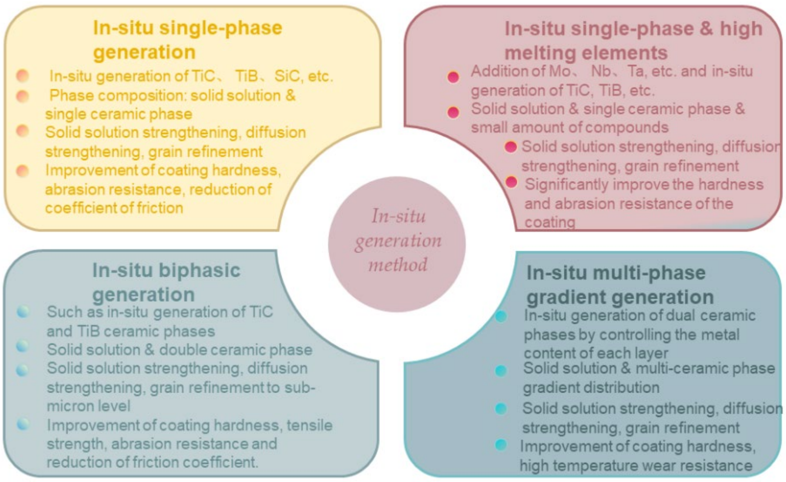

Figure 6. Summary of in situ generation method.

2.2. Addition Method

The additive method involves mixing ceramic powder and high-entropy alloy powder according to a certain proportion, ball milling the mixture, and pre-positioning it on the surface of the substrate. Alternatively, synchronous powder delivery can be used under the protection of inert gas or in a vacuum environment using a laser heat source to melt the pre-positioned coatings or spray powder, so that the powder into the metal substrate surface to form a ceramic phase reinforced by the high-entropy alloy coatings. The pre-positioning method is commonly used in experimental protocols where the powder particles are on the nano-scale, and the simultaneous powder feeding is mostly used for mixed powders of tens of microns or more.

The external addition method allows for the accurate control of the size and content of ceramic particles in high-entropy alloy composite coatings compared to the in situ generation method. Wang et al. [48], Li et al. [49], and Xi et al. [50] discovered that a small number of small-sized ceramic particles can greatly refine the grain size of the target material and effectively enhance its mechanical properties. Cai et al. [51] conducted an investigation on the laser fusion coating of FeMnCrNiCo + x(TiC) (x = 0, 5, 10, 15 wt%) coatings. The experiments involved adding a mixture of TiC ceramic particles with particle sizes ranging from 10 μm to 20 μm. This study shows that the joint action of TiC ceramic particles with small-size particles (SSP), large-size particles (LSP), and precipitation phase at the grain boundary can refine the metal grains of the coating. The average grain size in the CoCrNiMn fusion cladding layer is 75.881 μm. However, with the addition of x = 0, 5, 10, 15 wt% TiC ceramic particles, the average grain size decreases to 36.061 μm, 29.714 μm, and 25.706 μm, respectively. This grain refinement significantly improves the resistance to plastic deformation of the fusion cladding layer. It is important to note that the plastic deformation resistance of the fusion-coated layer is significantly improved. However, as the ceramic content increases, coating cracks tend to extend along the grain direction. Additionally, excessive ceramic content during the friction process can accelerate the detachment of ceramic particles from the surface of the coating. Li et al. [52], in order to further improve the hardness and abrasion resistance of the AlCoCrFeNi high-entropy alloy, investigated the effect of different ceramic contents on the performance of the high-entropy coatings. Experiments in the AlCoCrFeNi high-entropy alloy with different mass fractions (10%, 20%, 30%) of NbC ceramic particles were added, and the coatings were prepared using the laser cladding method to study the organizational evolution and mechanical behaviors of the composite coatings with different contents of NbC particles. NbC particles are mainly distributed in the grain boundaries of the high-entropy alloys, and the NbC particles have a strong pinch effect, which has unique advantages in inhibiting the growth of high-entropy alloys' grains. NbC particles have a strong pinch effect, which has a unique advantage in inhibiting the grain growth of high-entropy alloys, and the FCC phase in the coating decreases as the content of NbC particles increases. When the mass fraction of NbC particles is 20%, the alloy has the highest hardness (525 HV), the best wear resistance with an average coefficient of friction value of 1.023, and a mass loss of 1.05 mg. The additive method allows for a flexible selection of ceramic particles, overcoming the limitations of the in situ generation method. SiC is an excellent ceramic reinforcement because of its high hardness, excellent wear resistance, superior thermal conductivity, and high-temperature oxidation resistance; it is often selected as the reinforcing phase for metallic materials. Xu et al. [53] prepared SiC particle-reinforced CoCrFeNiCu composite coatings on the surface of 316 L stainless steel using the laser melting technique. The CoCrFeNiCu $(SiC)_x$ HEA coating is a face-centered cubic structure, and a second phase consisting of Cr_7C_3 is formed at the grain boundaries. Grain boundary strengthening improves the hardness, wear resistance, and corrosion resistance. For the CoCrFeNiCu $(SiC)_{15}$ HEA coating, the microhardness, wear, and friction coefficients were 568.4 HV, 0.9 mg, and 0.35, respectively. With the increase of SiC content, the corrosion resistance of CoCrFeNiCu $(SiC)_x$ HEA coatings in 3.5% NaCl solution increases. The corrosion performance of the CoCrFeNiCu $(SiC)_{1.0}$ coatings is better than the other coatings, and the wear resistance, tribological properties, and corrosion resistance of CoCrFeNiCu high-entropy alloy with the addition of SiC ceramic phase are significant. The wear resistance, tribological properties, and corrosion resistance of CoCrFeNiCu high-entropy alloy with SiC ceramic phase are significantly improved. In the high-entropy alloy composite coatings with added ceramics, changes in the atomic ratio of certain constituent elements in the high-entropy alloy base will cause a phase change in the coating and thus improve the coating properties and the effect of changes in the atomic ratio in the high-entropy coatings on the properties of the composite coatings can be conveniently realized by the additive method. Xu et al. [54] investigated the effect of the content of Al and Ti on the properties of the AlCoCrFeNiTi HEA coatings reinforced by SiC particles under laser melting conditions. The influence of

Al and Ti element content on the characteristics of AlCoCrFeNiTi coatings reinforced with SiC particles under laser melting conditions was examined. The microstructures, phase compositions, mechanical properties, and corrosion resistance of the coatings with and without SiC particles were analyzed and compared, offering novel research to elucidate the advancement of high-strength and high-wear-resistant high-entropy alloy coatings. The results show that SiC particles decompose into Si and C during liquid phase deposition. The cubic phase L_{21} in the $Al_{0.5}$ alloy coatings precipitates out of the disordered BCC matrix and transforms into the coarse lath-like organization composed of the L_{21} and FCC matrix in the $Al_{0.5}$/SiC coatings. Meanwhile, the braided network structure in the $Al_{0.8}$/SiC alloy coatings was more refined with the increase of the volume fraction of the B2 phase. The hardness of the $Al_{0.8}$/SiC alloy coatings increased from 637 $HV_{0.2}$ to 718 $HV_{0.2}$, and the coefficient of friction was reduced from 0.40 to 0.31. The presence of SiC particles exerted a detrimental impact on the microhardness of the $Al_{0.5}$/SiC alloy coating, leading to a decrease from 743 $HV_{0.2}$ to 679 $HV_{0.2}$. This was attributed to the coarsening of the microstructure and an increased fraction of the supple FCC solid solution. The formation of a fine cubic L_{21} phase in the disordered BCC matrix in the $Al_{0.5}$ alloy coatings was replaced by a lath-like coupled organization consisting of FCC and L_{21} phases. As a result, the coating microhardness shows a decreasing trend.

High-content ceramic particles reinforced laser fusion composite coatings are brittle and generate huge thermal stresses during the laser fusion process, which often leads to the presence of cracks. The selection and design of metal matrix materials is an effective way to solve the cracking problem of metal–ceramic composite coatings. Due to the special composition design, high-entropy alloys (HEAs) have excellent wear resistance, corrosion resistance, and high-temperature softening resistance. In particular, HEAs with face-centered cubic (FCC) single solid-phase structures exhibit good toughness and corrosion resistance but low hardness and strength. Combining FCC HEAs with ceramic particles can obtain composite coatings with high strength and toughness. Ma et al. [55] successfully prepared a crack-free 60 wt% WC particle-reinforced FeCoNiCr high-entropy alloy composite coating. The composite coating consists of a face-centered cubic (FCC) solid-solution phase, WC, W_2C, and Co_4W_2C. The composite coating consists of dendrites, massive precipitated phases, and herringbone-like precipitated phases distributed around the WC particles. The composite coating has no obvious weaving structure. The average microhardness of the composite coatings was 506 $HV_{0.05}$. The average coefficient of friction and wear volume loss were 0.474 and 0.041 mm^3, respectively, significantly improving the coatings' hardness and wear resistance.

When the physical properties of the ceramic particles and the alloy matrix are different, increasing residual stresses within the coating as the ceramic addition increases can lead to cracks within the coating. According to studies [56–60], the best option to reduce residual stresses and enhance wear and corrosion performance is to use gradient coatings with continuous compositional content variations. Functional gradient coatings on ceramic and metallic materials lead to coatings with continuous gradient behavior in terms of organization and properties. These coatings meet the specific performance requirements at different locations of the part and address the defects associated with poor bond strength and rapid changes in properties at the metal/ceramic interface. Wang et al. [61] and Chen et al. [62] showed that gradient coatings improve the performance of ceramic composite coatings to a large extent and provide new ideas for surface modification and repair of parts. Zhang et al. [63] explored a new method of ceramic-reinforced $CoCrFeNiMo_{0.2}$ high-entropy alloy composite gradient coating in order to strengthen the high-entropy alloy with a face-centered cubic structure, and the design of the coating on the substrate surface. SiC was not added to the first layer of material to improve the bonding strength between the coating and the matrix, and the SiC content was increased layer by layer. Process optimization parameters were used, and each layer was cooled for three minutes after fusion coating to reduce heat accumulation. The cross-sectional SEM images of the gradient coatings are shown in Figure 7, with good bonding between the coating and the substrate and between the coating and the interlayer, no cracks within the coating, and obvious porosity in the fourth layer, and the morphology of the coatings is directly correlated with the increase in SiC content. When a high-power laser melts, silicon carbide mainly decomposes into graphite and silicon vapor. Some carbon atoms dissolve in the solid solution, while others combine with other alloying elements to form carbides. Excessive decomposition of silicon carbide leads to an excess of elemental carbon. In a high-temperature melt pool, the carbon adsorbs to each other and covers the gaseous material, slowing down the release of the gas. The melt pool solidifies rapidly, and the gases have no time to escape. As a result of the pressure, a structure with large pores on the coating and small pores underneath is eventually formed. The gradient coatings prepared using this method possessed good frictional and mechanical properties, with the second, third, and fourth layers exhibiting significantly higher average hardnesses, measured at 594 HV, 722 HV, and 788 HV, respectively, which can be attributed to the presence of a body-centered cubic structure, carbides, and grain-boundary strengthening effects. The hardness of these layers is three to four times higher than that of the first layer. The wear mechanism changes from adhesive wear to abrasive wear as the number of coating layers increases. The wear rates of the second, third, and fourth layers were all reduced by at least 87% compared to the first layer. However, different forms of abrasive wear were observed between these layers. The results of this study have important engineering implications.

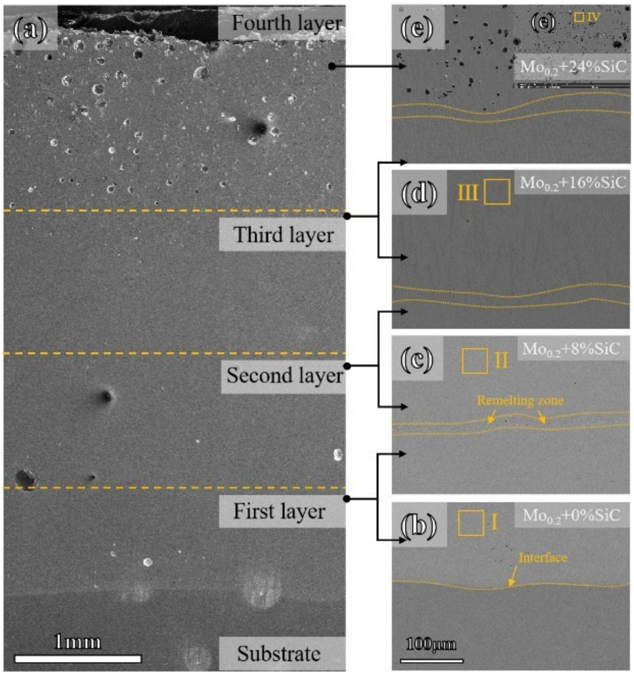

Figure 7. (**a**) full view of the cross section of the gradient coating; (**b**) the bonding area between the substrate and the coating; (**c**) combined area of the first and second layers; (**d**) combined area of the second and third floors; (**e**) combined area of the third and fourth floors [63].

The additive method is currently focused on the high-entropy alloy to add a ceramic phase, high-entropy alloy of certain elements in the change on the addition of ceramic phase after the coating performance, gradient composite coatings, and other research methods as shown in Figure 8, each method of ceramic particles added to the content and size of the different will have an impact on the coating organization and thus affecting the performance of the coating. Compared to the in situ generation method, the additive method can flexibly control the size and content of ceramic particles in the coating. Although the coating obtained via the additive method is easy to produce micro-cracks along the direction of the ceramic particles, via the control of the ceramic content, particle size, and process parameters, it can effectively control the cracks produced by the coating to obtain excellent performance.

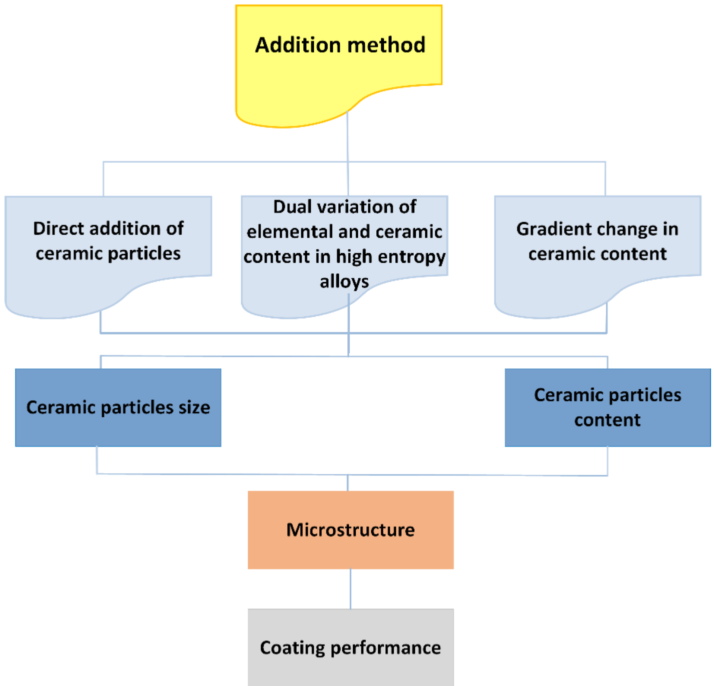

Figure 8. Summary chart of additive method studies.

3. Discussion

There are many factors affecting the surface quality and coating properties of high-entropy alloy composite coatings, which can be mainly classified into three categories. As shown in Figure 9, the first category is the laser process parameters and laser characteristics, such as laser power, spot size, focal length and laser wavelength, beam profile, polarization, and so on. The second category is the substrate surface parameters such as protective gas, scanning path, scanning speed, lap rate, and preheating and heat treatment of the substrate. The third category is the properties of high-entropy alloy composite coatings. The method of introducing ceramic particles, the size of ceramic particles, the content of ceramic particles in the high-entropy coating, and the uniformity of ceramic particles within the coating all have a non-negligible effect on the properties of high-entropy alloy composite coatings. This paper focuses on the collation and in-depth discussion of the influence of the third category of influencing factors on the microstructure and macroscopic properties of ceramic phase-reinforced high-entropy alloy composite coatings. The main approaches for preparing ceramic phase-reinforced high-entropy alloy composite coatings using the laser melting method are the in situ generation method and additive method. The in situ generation method utilizes laser thermal energy to generate the ceramic phase by chemical reaction in situ. The ceramic phase obtained is uniformly distributed, and the coating forms a good metallurgical bond with the substrate, which can reduce the stress concentration on the coating, thus effectively reducing the phenomena of coating cracking and ceramic particle detachment. The ceramic particles synthesized by this method are much finer, which can effectively prevent the growth of grain branching and thus refine the grains. However, it is difficult to control the content of ceramic particles in the coating by the in situ generation method, making it challenging to obtain high-entropy alloy coatings with high ceramic content. Compared with the in situ generation method, the addition method shows a more controllable coating composition, which enables to obtain high-entropy alloy coatings with high ceramic content, and the size of ceramic particles in the coatings can be precisely controlled. However, it is prone to phenomena such as cracks and micropores inside the coating, which makes it difficult to obtain uniformly distributed ceramic particles. In general, selecting the appropriate preparation method based on the properties of the desired coating can effectively minimize coating defects and result in a high-quality coating. Overall, the specific choice of preparation method needs to be rationally selected according to the performance of the desired coating so as to obtain a high-quality coating. Based on the above discussion, we further summarized the data in the reported literature on the effect of coating preparation methods on the microstructure and properties of coatings, as shown in Table 1.

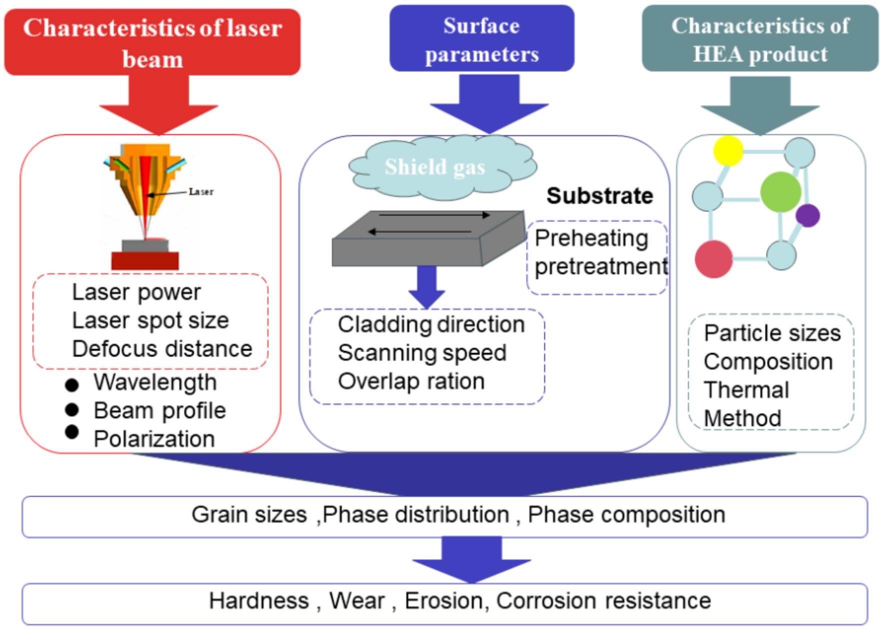

Figure 9. Factors affecting ceramic phase-reinforced high-entropy alloy composite coatings.

Table 1. Overview of process parameters, HEA compositions, ceramic particles, microstructures, and major properties.

Preparation Method	Process Parameters	Substrate Materials	HEAs	Ceramic Particles	Phase (Minor–Major)	Optimal Performance	Ref.
	LP 1500 W SR 7.5 mm/s SD 3 mm OR 40%	304 stainless steel	$CoCrCuFeNiSi_{0.2}$	TiC	FCC,TiC	H = 498.5 HV WV = 0.42 mm^3	[31]
	LP 2400 W SR 5 mm/s SD4.6 mm OR 40%	AISI 1045 steel	AlCoCrFeNiTix (x = 0, 0.2, 0.4, 0.6, 0.8, 1.0)	TiC	Two BCC,TiC	H = 860.1 HV HWR = 5.8 × 10^{-8} $mm^3N^{-1}m^{-1}$	[32]
	LP 1500 W SR 5 mm/s SD 3 mm OR 35%	Ti-6Al-4 V titanium alloy	CoCrMoNbTi	TiC	BCC_1 and BCC_2,TiC	H = 886.9 HV WR = 3.83 × 10^{-4} $mm^3N^{-1}m^{-1}$	[34]
In situ	LP 1000 W SR 18 mm/s SD 35 mm OR 30%	Q235 steel	AlCoCrFeNi	Mo,TiC	BCC,TiC,	H = 1006.3 HV E_r = 243.3 Gpa	[39]
	LP 1500 W SR 5 mm/s SD 3 mm OR 35%	Ti-6Al-4V titanium alloy	CoCrMoNbTi	TiC,TiB	BCC,TiC,TiB	H = 954.11 HV E_r = 240.35 Gpa	[45]
	LP 600 W SR 8 mm/s SD 1 mm	H13 steel	AlCoCrFeNiSi	Ti(C, N)	FCC,BCC,B_2	H = 934 HV WL = 12 mg	[46]
	LP 1500 W SR 800 mm/min SD 2 mm	Ti-6Al-4V titanium alloy	MoNbTaW	TiN/(Nb, $Ti)_5Si_3$	TiN/(Nb, $Ti)_5Si_3$,BCC	H = 628.07 HV WV = 0.95× 10^{-7} um^3	[64]

Table 1. *Cont.*

Preparation Method	Process Parameters	Substrate Materials	HEAs	Ceramic Particles	Phase (Minor–Major)	Optimal Performance	Ref.
Addition	LP 1300 W SR 5 mm/s SD 3 mm OR 30%	4Cr5MoSiV1 die steel	FeMnCrNiCo	TiC	FCC,TiC	H = 288.3 HV	[51]
	LP 2500 W SR 4 mm/s SD 3 mm OR 30%	Q235 steel	AlCoCrFeNi	NbC	FCC,BCC,NbC	H = 525 HV WL = 12 mg FC = 1.023	[52]
	LP 2000 W SR 180 mm/min SD 20.4 mm	316 L stainless steel	CoCrFeNiCu	SiC	FCC,SiC,Cr_7C_3	H = 563.4 HV Ba = 471.6 mv CR = 0.040087 mm/a	[53]
	LP 2000 W SR 11 mm/s SD 4 mm	AISI1045 steel	AlxCoCrFeNiTi1-x	SiC	FCC,BCC,$L2_1$-Ni_2AlTi	H = 743 HV FC = 0.31	[54]
	LP 1600 W SR 10 mm/s SD 4 mm OR 50%	316 L stainless steel	FeCoNiCr	WC	FCC,WC,W_2C,Co_4W_2C	H = 506 HV WV = 0.041	[55]
	LP 2100 W SR 800 mm/s SD 3 × 3 mm	45 steel	$CoCrFeNiMo_{0.2}$	SiC	FCC,BCC,$M_{23}C_6$,M_7C_3	H = 788 HV	[63]
	LP 1300 W SR 6 mm/s SD 3 mm OR 30%	304 stainless steel	CrMnFeCoNiM (M = TiC, NbC, B4C)	TiC, NbC, B_4C	TiC:FCC,TiC NbC:FCC,NbC B4C:M_2B, $M_{23}C_6$,FCC	COF = 0.15–0.25	[65]

The elements Co, Cr, Fe, and Ni have similar atomic radii, which make it easy to form a single FCC or BCC phase. The BCC phase shows high strength and hardness but poor toughness; and the FCC phase presents high plasticity but low hardness. Many scholars introduced the elements Al, Ti, Mo, and V with large atomic radii into this alloy system to enhance the lattice distortion of high-entropy alloys, thus promoting the generation of the BCC phase. On the basis of this high-entropy alloy system, the introduction of ceramic particles using different preparation methods may effectively improve the properties of high-entropy alloys, such as hardness and wear resistance. It is clear from Table 1 that in the use of in situ generation method to obtain ceramic particles, most scholars adopt the introduction of non-metallic elements such as C, N, B, etc., which form trace intermetallic compounds with Ti elements in situ and are uniformly distributed in the coatings with the effect of dispersion strengthening, solid-solution strengthening, and grain refining, and thus significantly improve the hardness, abrasion resistance, and plastic deformation resistance of the coatings. As for the addition method, it mostly focuses on the introduction of ceramic particles such as SiC, TiC, NbC, B4C, and WC. Since the addition method is flexible in controlling the content of ceramic particles in the coating, the ceramic content in the coating is usually higher than that of the in situ generation method, thus obtaining coatings with higher hardness and better abrasion resistance.

Regarding the preparation of high-entropy alloy composite coatings using the laser cladding method, although it has the characteristics of small deformation, high densification, low dilution rate, and good metallurgical bonding, there are still some minor deficiencies at present. The coatings prepared using the laser cladding method usually have four kinds of defects: cracks, porosity, residual stress, and rough casting organization with high chemical inhomogeneity. These phenomena have a non-negligible impact on the coating's quality and properties, and we need to adopt certain methods to reduce the defects in the preparation of high-entropy alloy composite coatings. Therefore, on the basis of choosing a suitable method of introducing ceramic particles, laser cladding defects can be reduced or eliminated in four ways. As shown in Figure 10, the main cause of cracks in the coating is the high-temperature gradient between the cladding and the substrate. Most authors have investigated the effect of heating the substrate prior to laser cladding on the quality of the coating, and positive results have been observed [66]. Liu et al. [32] obtained good quality high-entropy alloy composite coatings by preheating the substrate at 200 degrees Celsius when preparing TiC-reinforced AlCoCrFeNi high-entropy alloy composite coatings. Therefore, the preheating treatment of the substrate before fusion coating can effectively alleviate the phenomenon of cracking of the coating with high thermal stress after fusion coating. Then, in order to improve the metallurgical bonding between the coating and the substrate, many scholars have tried to introduce an intermediate layer between the substrate and the coating to reduce the residual stress and improve the cracking phenomenon. This provides new design ideas to enhance the quality of the prepared composite coatings and reduce coating defects. At the same time, the selection of appropriate laser cladding parameters via experiments has an important reference value for improving the defects on the inner surface of the coating.

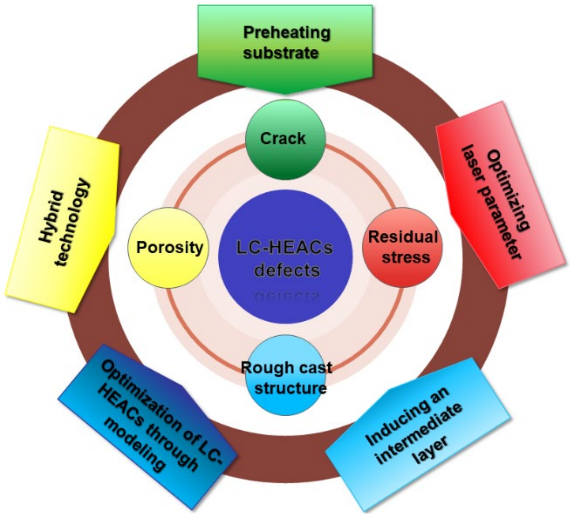

Figure 10. LC-HEAs defects and eliminates the problems of laser cladding methods.

An appropriate scanning strategy and suitable process parameters are crucial for obtaining crack-free microstructures. The laser process parameters mainly include laser power, laser scanning speed, spot diameter, powder delivery, lap rate, preset coating thickness, etc., among which the laser power and scanning speed are the main factors affecting the coating quality. The majority of research has concentrated on investigating the impact of laser process parameters on the coating properties of high-entropy alloys, with limited attention given to the exploration of laser process parameters on the coating properties of high-entropy alloys reinforced with ceramic phases. The optimal scanning power and scanning speed based on different systems in the existing literature are summarized as shown in Figure 11, which shows that the optimal laser power concentrates between 1300 and 2000 W and the optimal scanning speed lies in the range of 5–14 mm/s [31,32,34,39,45,46,51–55,64]. Therefore, this range may provide a reference for the selection of process parameters for the subsequent laser cladding process. With the development of simulation software, laser cladding process parameters can be optimized by cladding process simulation, which provides a reference for selecting the best process parameters. To improve the phenomena of elemental segregation, rough cast structure with high chemical heterogeneity, and porosity inclusions in the coating, hybrid technology is needed in the cladding process. Wen et al. [67] used a combination of substrate preheating and ultrasonic-assisted technology to obtain FeCrCoAlMn0.5Mo0.1-based HEACs with no defects and good wear and corrosion resistance. At the same time, the heat treatment technology for the high-entropy alloy composite coating after cladding can effectively diminish the grain boundary anti-cracking sensitivity and improve the wear resistance of the coating. Meanwhile, the heat treatment process of ceramic phase-reinforced high-entropy alloy coating is less studied, and the organizational evolution of ceramic phase-reinforced high-entropy alloy composite coatings via the heat treatment process is still uncertain; these directions are the focus of = future research on composite high-entropy alloy coatings.

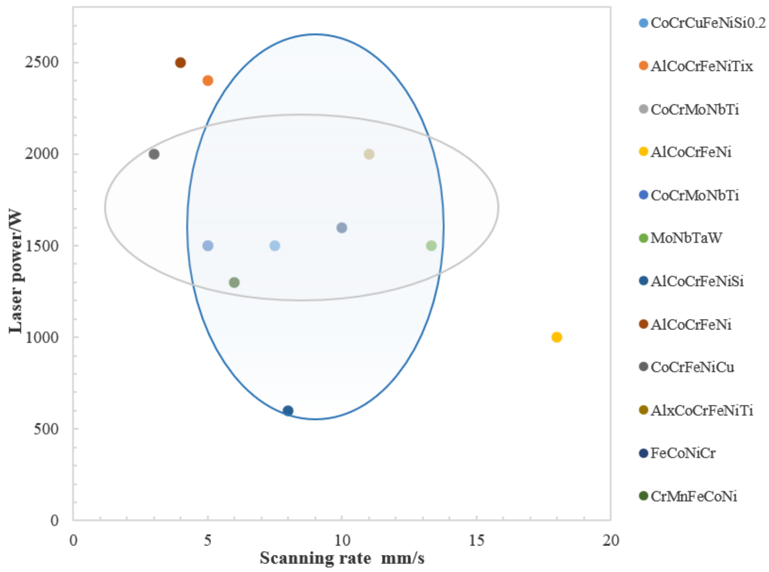

Figure 11. Power and scanning speed of ceramic phase-reinforced high-entropy alloy composite coatings.

4. Conclusions

Ceramic phase-reinforced high-entropy alloy composite coatings show excellent hardness, abrasion resistance, corrosion resistance, and high-temperature oxidation resistance, which may improve the service life of mechanical equipment and has broad industrial application prospects. In recent years, more and more researchers have committed to the study of high-entropy alloy composite coatings, but high-entropy alloy composite coatings are still in the primary stage of development. This paper reviewed the current research results, and the future developments of high-entropy alloy composite coatings are summarized as follows:

(1) Simulation research of high-entropy alloy composite coating. The current simulation of high-entropy alloy coating is primarily based on first principle calculation, molecular dynamics simulation, and phase diagram calculation. These methods aim to predict the formation behavior of high-entropy alloy and simulate the melting process of the coating. However, the existing simulation software lacks accuracy in simulating the coupling of multiple physical fields (such as temperature, fluid, and stress) during the laser melting and cladding of high-entropy alloy composite coatings. Additionally, it does not have a comprehensive selection of coating materials, including powder particle size and preparation process. As a result, most research on high-entropy alloy composite coatings still relies on repeated experiments. To overcome these limitations, it is necessary to enhance the simulation software by introducing new options for material parameters and preparation processes. This will enable a flexible, efficient, and cost-effective research and development process.

(2) High-entropy alloy composite coatings in extreme conditions. Existing research on the performance of ceramic phase-reinforced high-entropy alloy composite coatings mostly focuses on mechanical properties, friction properties, and electrochemical corrosion properties at room temperature. Research on extreme conditions such as thermal fatigue performance, ultra-low temperature performance, irradiation resistance, and other properties is less. Via the study of its performance under extreme conditions, it is expected to be applied to the surface protection of key components under special conditions, such as aerospace turbine blades, oil drilling parts, biomedical fields, superconducting materials, etc.

(3) New process research. Ceramic phase-reinforced high-entropy alloy composite coatings are prone to defects such as porosity and cracks in the coating during laser melting and cladding. The development of new processes such as laser–ultrasonic

vibration composite, electric field–magnetic field synergism, and other multi-physical field composite processing processes can effectively mitigate the generation of coating defects. Obtaining high-quality coatings via new processes may facilitate industrialized production applications.

(4) The study of different kinds of ceramic contents and self-lubricating phases in high-entropy alloy composite coatings. With the increase of ceramic content in high-entropy alloys or the mismatch between the selected ceramic phase and the high-entropy alloy system, will lead to defects such as porosity and cracks in the fusion coating process. This is due to differences in chemical potentials, thermal coefficients of linear expansion, etc. A self-lubricating phase is usually introduced to improve coating defects. Thus, it is of great interest to further investigate the different types of ceramic contents and suitable self-lubricating phases in composite coatings to improve coating defects.

Author Contributions: Conceptualization, H.Z. and Y.Y.; methodology, H.L., Y.G., H.Z. and F.W.; investigation, Y.L., L.L. and H.Z.; writing, review, and editing, H.Z. and L.L.; visualization, H.L. and Y.G.; supervision, Y.Y.; funding acquisition, H.L. and Y.G. All authors have read and agreed to the published version of the manuscript.

Funding: This research was funded by [the Ningxia Natural Science Foundation] grant number [No. 2023AAC02047], [the National Science Foundation of China] grant number [No. 51165019], [the Ningxia Engineering Research Center for Hybrid Manufacturing System Foundation] grant number [No. 2023GCJS008] And [Ningxia Key Research and Development Program (Special Talents)] grant number [2020BEB04030].

Institutional Review Board Statement: Not applicable.

Informed Consent Statement: Not applicable.

Data Availability Statement: No new data were created or analyzed in this study. Data sharing is not applicable to this article.

Conflicts of Interest: The authors declare no conflicts of interest.

References

1. Zhang, Y.; Zhou, Y.J.; Lin, J.P.; Chen, G.L.; Liaw, P.K. Solid-Solution Phase Formation Rules for Multi-component Alloys. *Adv. Eng. Mater.* **2008**, *10*, 534–538. [CrossRef]
2. Yeh, J.-W.; Chen, S.-K.; Lin, S.-J. Nanostructured Hight-Entropy Alloys with Multiple Principal Elements: Novel Alloy Design Concepts and Outcomes. *Adv. Eng. Mater.* **2004**, *6*, 299–303. [CrossRef]
3. Cantor, B.; Chang, I.T.H.; Knight, P.; Vincent, A.J.B. Microstructural development in equiatomic multicomponent alloys. *Mater. Sci. Eng. A* **2004**, *375–377*, 213–218. [CrossRef]
4. Yeh, J.W.; Chen, Y.L.; Lin, S.J.; Chen, S.K. High-Entropy Alloys—A New Era of Exploitation. *Mater. Sci. Forum* **2007**, *560*, 1–9. [CrossRef]
5. Zhang, Y.; Zuo, T.T.; Tang, Z.; Gao, M.C.; Dahmen, K.A.; Liaw, P.K.; Lu, Z.P. Microstructures and properties of high-entropy alloys. *Prog. Mater. Sci.* **2014**, *61*, 1–93. [CrossRef]
6. Liu, K.; Komarasamy, M.; Gwalani, B.; Shukla, S.; Mishra, R.S. Fatigue behavior of ultrafine grained triplex $Al_{0.3}CoCrFeNi$ high entropy alloy. *Scr. Mater.* **2019**, *158*, 116–120. [CrossRef]
7. Wang, W.; Wang, J.; Sun, Z.; Li, J.; Li, L.; Song, X.; Wen, X.; Xie, L.; Yang, X. Effect of Mo and aging temperature on corrosion behavior of $(CoCrFeNi)_{100-x}Mo_x$ high-entropy alloys. *J. Alloys Compd.* **2020**, *812*, 152139. [CrossRef]
8. Chuang, M.-H.; Tsai, M.-H.; Wang, W.-R.; Lin, S.-J.; Yeh, J.-W. Microstructure and wear behavior of $AlxCo_{1.5}CrFeNi_{1.5}Tiy$ high-entropy alloys. *Acta Mater.* **2011**, *59*, 6308–6317. [CrossRef]
9. Li, Y.; Shi, Y. Microhardness, wear resistance, and corrosion resistance of AlxCrFeCoNiCu high-entropy alloy coatings on aluminum by laser cladding. *Opt. Laser Technol.* **2021**, *134*, 106632. [CrossRef]
10. Rogal, Ł.; Kalita, D.; Tarasek, A.; Bobrowski, P.; Czerwinski, F. Effect of SiC nano-particles on microstructure and mechanical properties of the CoCrFeMnNi high entropy alloy. *J. Alloys Compd.* **2017**, *708*, 344–352. [CrossRef]
11. Yang, J.; Liu, W.; Fu, M.; Wen, J.; Li, K.; Lin, P.; Wang, C.; He, P.; Lin, T.; Mei, H.; et al. Joining SiCf/SiC composites to $Al_{0.3}CoCrFeNi$ high-entropy alloys with a Cu–Ti filler alloy: Interfacial reactions, high-entropy effects, and mechanical properties. *Mater. Sci. Eng. A* **2023**, *881*, 145390. [CrossRef]
12. Liu, S.; Wang, Y.; Muthuramalingam, T.; Anbuchezhiyan, G. Effect of B_4C and MOS_2 reinforcement on micro structure and wear properties of aluminum hybrid composite for automotive applications. *Compos. Part B Eng.* **2019**, *176*, 107329. [CrossRef]

13. Arif, Z.U.; Khalid, M.Y.; ur Rehman, E.; Ullah, S.; Atif, M.; Tariq, A. A review on laser cladding of high-entropy alloys, their recent trends and potential applications. *J. Manuf. Process.* **2021**, *68*, 225–273. [CrossRef]
14. Yang, S.; Yan, X.; Yang, K.; Fu, Z. Effect of the addition of nano-Al_2O_3 on the microstructure and mechanical properties of twinned $Al_{0.4}FeCrCoNi_{1.2}Ti_{0.3}$ alloys. *Vacuum* **2016**, *131*, 69–72. [CrossRef]
15. Braic, M.; Braic, V.; Vladescu, A.; Zoita, C.N.; Balaceanu, M. Solid solution or amorphous phase formation in TiZr-based ternary to quinternary multi-principal-element films. *Prog. Nat. Sci. Mater. Int.* **2014**, *24*, 305–312. [CrossRef]
16. Ji, X.; Duan, H.; Zhang, H.; Ma, J. Slurry Erosion Resistance of Laser Clad $NiCoCrFeAl_3$High-Entropy Alloy Coatings. *Tribol. Trans.* **2015**, *58*, 1119–1123. [CrossRef]
17. Yao, C.-Z.; Zhang, P.; Liu, M.; Li, G.-R.; Ye, J.-Q.; Liu, P.; Tong, Y.-X. Electrochemical preparation and magnetic study of Bi–Fe–Co–Ni–Mn high entropy alloy. *Electrochim. Acta* **2008**, *53*, 8359–8365. [CrossRef]
18. Yue, T.; Xie, H.; Lin, X.; Yang, H.; Meng, G. Microstructure of Laser Re-Melted AlCoCrCuFeNi High Entropy Alloy Coatings Produced by Plasma Spraying. *Entropy* **2013**, *15*, 2833–2845. [CrossRef]
19. Mu, Y.; Zhang, L.; Xu, L.; Prashanth, K.; Zhang, N.; Ma, X.; Jia, Y.; Xu, Y.; Jia, Y.; Wang, G. Frictional Wear and Corrosion Behavior of AlCoCrFeNi High-Entropy Alloy Coatings Synthesized by Atmospheric Plasma Spraying. *Entropy* **2020**, *22*, 740. [CrossRef]
20. Cai, Y.; Zhu, L.; Cui, Y.; Geng, K.; Manladan, S.M.; Luo, Z.; Han, J. Strengthening mechanisms in multi-phase $FeCoCrNiAl_{1.0}$ high-entropy alloy cladding layer. *Mater. Charact.* **2020**, *159*, 110037. [CrossRef]
21. Sun, S.; Durandet, Y.; Brandt, M. Parametric investigation of pulsed Nd: YAG laser cladding of stellite 6 on stainless steel. *Surf. Coat. Technol.* **2005**, *194*, 225–231. [CrossRef]
22. Menghani, J.; Vyas, A.; Patel, P.; Natu, H.; More, S. Wear, erosion and corrosion behavior of laser cladded high entropy alloy coatings—A review. *Mater. Today Proc.* **2021**, *38*, 2824–2829. [CrossRef]
23. Liu, Y.; Xiang, D.; Wang, K.; Yu, T. Corrosion of Laser Cladding High-Entropy Alloy Coatings: A Review. *Coatings* **2022**, *12*, 1669. [CrossRef]
24. Cheng, W.; Ji, L.; Zhang, L.; Wang, H.; Sun, W. Refractory high-entropy alloys fabricated using laser technologies: A concrete review. *J. Mater. Res. Technol.* **2023**, *24*, 7497–7524. [CrossRef]
25. Xie, H.; Tong, Y.; Bai, Y.; Li, X.; Han, Y.; Hua, K.; Wang, H. Wear-Resistance of High-Entropy Alloy Coatings and High-Entropy Alloy-Based Composite Coatings Prepared by the Laser Cladding Technology: A Review. *Adv. Eng. Mater.* **2023**, *25*, 2300426. [CrossRef]
26. Kołodziejczak, P.; Bober, M.; Chmielewski, T. Wear Resistance Comparison Research of High-Alloy Protective Coatings for Power Industry Prepared by Means of CMT Cladding. *Appl. Sci.* **2022**, *12*, 4568. [CrossRef]
27. Liang, J.; Yin, X.; Lin, Z.; Chen, S.; Liu, C.; Wang, C. Microstructure and wear behaviors of laser cladding in-situ synthetic (TiBx+TiC)/(Ti_2Ni+TiNi) gradient composite coatings. *Vacuum* **2020**, *176*, 109305. [CrossRef]
28. Feng, Y.; Feng, K.; Yao, C.; Li, Z.; Sun, J. Microstructure and properties of in-situ synthesized (Ti_3Al + TiB)/Ti composites by laser cladding. *Mater. Des.* **2018**, *157*, 258–272. [CrossRef]
29. Yang, L.; Yu, T.; Li, M.; Zhao, Y.; Sun, J. Microstructure and wear resistance of in-situ synthesized Ti(C, N) ceramic reinforced Fe-based coating by laser cladding. *Ceram. Int.* **2018**, *44*, 22538–22548. [CrossRef]
30. Lin, Y.; Jiang, C.; Lin, Z.; Chen, Q.; Lei, Y.; Fu, H. Laser in-situ synthesis of high aspect ratio TiB fiber bundle reinforced titanium matrix composite coating. *Opt. Laser Technol.* **2019**, *115*, 364–373. [CrossRef]
31. Guo, Y.; Li, C.; Zeng, M.; Wang, J.; Deng, P.; Wang, Y. In-situ TiC reinforced $CoCrCuFeNiSi_{0.2}$ high-entropy alloy coatings designed for enhanced wear performance by laser cladding. *Mater. Chem. Phys.* **2020**, *242*, 122522. [CrossRef]
32. Liu, H.; Liu, J.; Chen, P.; Yang, H. Microstructure and high temperature wear behaviour of in-situ TiC reinforced AlCoCrFeNi-based high-entropy alloy composite coatings fabricated by laser cladding. *Opt. Laser Technol.* **2019**, *118*, 140–150. [CrossRef]
33. Zhou, X.; He, L.; Zhang, M.; Wang, P. Effect of ceramic particles on microstructure and properties of CoCrMoNbTi high-entropy alloy coating fabricated by laser cladding. *Optik* **2023**, *285*, 170987. [CrossRef]
34. Zhu, J.M.; Fu, H.M.; Zhang, H.F.; Wang, A.M.; Li, H.; Hu, Z.Q. Microstructures and compressive properties of multicomponent AlCoCrFeNiMox alloys. *Mater. Sci. Eng. A* **2010**, *527*, 6975–6979. [CrossRef]
35. Chang, R.; Fang, W.; Bai, X.; Xia, C.; Zhang, X.; Yu, H.; Liu, B.; Yin, F. Effects of tungsten additions on the microstructure and mechanical properties of CoCrNi medium entropy alloys. *J. Alloys Compd.* **2019**, *790*, 732–743. [CrossRef]
36. Xiang, K.; Chen, L.-Y.; Chai, L.; Guo, N.; Wang, H. Microstructural characteristics and properties of CoCrFeNiNbx high-entropy alloy coatings on pure titanium substrate by pulsed laser cladding. *Appl. Surf. Sci.* **2020**, *517*, 146214. [CrossRef]
37. Liu, H.; Gao, Q.; Dai, J.; Chen, P.; Gao, W.; Hao, J.; Yang, H. Microstructure and high-temperature wear behavior of $CoCrFeNiW_x$ high-entropy alloy coatings fabricated by laser cladding. *Tribol. Int.* **2022**, *172*, 107574. [CrossRef]
38. Li, Z.; Jing, C.; Feng, Y.; Wu, Z.; Lin, T.; Zhao, J. Microstructure evolution and properties of laser cladding Nb containing eutectic high entropy alloys. *Int. J. Refract. Met. Hard Mater.* **2023**, *110*, 105992. [CrossRef]
39. Zhao, W.; Yu, K.; Ma, Q.; Song, C.; Xiao, G.; Zhang, H.; Lv, Y.; Guo, N.; Li, Z. Synergistic effects of Mo and in-situ TiC on the microstructure and wear resistance of AlCoCrFeNi high entropy alloy fabricated by laser cladding. *Tribol. Int.* **2023**, *188*, 108827. [CrossRef]
40. Zhao, Y.; Yu, T.; Chen, L.; Chen, Y.; Guan, C.; Sun, J. Microstructure and wear resistance behavior of Ti–C–B_4C-reinforced composite coating. *Ceram. Int.* **2020**, *46*, 25136–25148. [CrossRef]

41. Ye, F.; Yang, Y.; Lou, Z.; Feng, L.; Guo, L.; Yu, J. Microstructure and wear resistance of TiC reinforced $AlCoCrFeNi_{2.1}$ eutectic high entropy alloy layer fabricated by micro-plasma cladding. *Mater. Lett.* **2021**, *284*, 128859. [CrossRef]
42. Patil, A.S.; Hiwarkar, V.D.; Verma, P.K.; Khatirkar, R.K. Effect of TiB2 addition on the microstructure and wear resistance of Ti-6Al-4V alloy fabricated through direct metal laser sintering (DMLS). *J. Alloys Compd.* **2019**, *777*, 165–173. [CrossRef]
43. Geng, L.; Ni, D.R.; Zhang, J.; Zheng, Z.Z. Hybrid effect of TiBw and TiCp on tensile properties of in situ titanium matrix composites. *J. Alloys Compd.* **2008**, *463*, 488–492. [CrossRef]
44. Song, R.; Li, J.; Shao, J.Z.; Bai, L.L.; Chen, J.L.; Qu, C.C. Microstructural evolution and wear behaviors of laser cladding Ti_2 Ni/α(Ti) dual-phase coating reinforced by TiB and TiC. *Appl. Surf. Sci.* **2015**, *355*, 298–309. [CrossRef]
45. He, L.; Zhang, M.; Wang, D.; Ye, X.; Zhou, Y.; Ruan, D.; Zhang, W. Microstructure and mechanical properties of in-situ dual ceramic phase synergistic strengthened $CoCrMoNbTi(B4C)_x$ high entropy alloy coating. *Opt. Laser Technol.* **2023**, *161*, 109172. [CrossRef]
46. Yan, G.; Zheng, M.; Ye, Z.; Gu, J.; Li, C.; Wu, C.; Wang, B. In-situ Ti(C, N) reinforced AlCoCrFeNiSi-based high entropy alloy coating with functional gradient double-layer structure fabricated by laser cladding. *J. Alloys Compd.* **2021**, *886*, 161252. [CrossRef]
47. Liu, S.S.; Zhang, M.; Zhao, G.L.; Wang, X.H.; Wang, J.F. Microstructure and properties of ceramic particle reinforced FeCoNiCrMnTi high entropy alloy laser cladding coating. *Intermetallics* **2022**, *140*, 107402. [CrossRef]
48. Wang, J.; Yang, H.; Huang, H.; Ruan, J.; Ji, S. Microstructure and mechanical properties of SiC whisker reinforced CoCrNi medium entropy alloys. *Mater. Lett.* **2019**, *254*, 77–80. [CrossRef]
49. Li, B.; Zhang, L.; Yang, B. Grain refinement and localized amorphization of additively manufactured high-entropy alloy matrix composites reinforced by nano ceramic particles via selective-laser-melting/remelting. *Compos. Commun.* **2020**, *19*, 56–60. [CrossRef]
50. Xi, L.; Gu, D.; Guo, S.; Wang, R.; Ding, K.; Prashanth, K.G. Grain refinement in laser manufactured Al-based composites with TiB_2 ceramic. *J. Mater. Res. Technol.* **2020**, *9*, 2611–2622. [CrossRef]
51. Cai, Y.; Zhu, L.; Cui, Y.; Shan, M.; Li, H.; Xin, Y.; Han, J. Fracture and wear mechanisms of FeMnCrNiCo + x(TiC) composite high-entropy alloy cladding layers. *Appl. Surf. Sci.* **2021**, *543*, 148794. [CrossRef]
52. Li, X.; Feng, Y.; Liu, B.; Yi, D.; Yang, X.; Zhang, W.; Chen, G.; Liu, Y.; Bai, P. Influence of NbC particles on microstructure and mechanical properties of AlCoCrFeNi high-entropy alloy coatings prepared by laser cladding. *J. Alloys Compd.* **2019**, *788*, 485–494. [CrossRef]
53. Xu, L.; Du, H.; Liu, J.; Feng, D.; Xia, S. Microstructure, Mechanical, and Electrochemical Properties of SiC Particle Reinforced CoCrFeNiCu High-Entropy Alloy Coatings. *Coatings* **2022**, *12*, 519. [CrossRef]
54. Xu, Y.; Wang, G.; Song, Q.; Lu, X.; Li, Z.; Zhao, Q.; Chen, Y. Microstructure, mechanical properties, and corrosion resistance of SiC reinforced $Al_xCoCrFeNiTi_{1-x}$ high-entropy alloy coatings prepared by laser cladding. *Surf. Coat. Technol.* **2022**, *437*, 128349. [CrossRef]
55. Ma, Q.; Lu, B.; Zhang, Y.; Wang, Y.; Yan, X.; Liu, M.; Zhao, G. Crack-free 60 wt% WC reinforced FeCoNiCr high-entropy alloy composite coating fabricated by laser cladding. *Mater. Lett.* **2022**, *324*, 132667. [CrossRef]
56. Taleghani, P.R.; Valefi, Z.; Ehsani, N. Evaluation of oxidation and thermal insulation capability of nanostructured $La_2(Zr_{0.7}Ce_{0.3})_2O_7$/YSZ functionally graded coatings. *Ceram. Int.* **2021**, *47*, 8915–8929. [CrossRef]
57. Sopronyi, M.; Nita, C.; Le Meins, J.-M.; Vidal, L.; Jipa, F.; Axente, E.; Matei Ghimbeu, C.; Sima, F. Laser-assisted synthesis of carbon coatings with cobalt oxide nanoparticles embedded in gradient of composition and sizes. *Surf. Coat. Technol.* **2021**, *419*, 127301. [CrossRef]
58. Li, L.; Wang, J.; Lin, P.; Liu, H. Microstructure and mechanical properties of functionally graded $TiCp/Ti_6Al_4V$ composite fabricated by laser melting deposition. *Ceram. Int.* **2017**, *43*, 16638–16651. [CrossRef]
59. Guévenoux, C.; Hallais, S.; Balit, Y.; Charles, A.; Charkaluk, E.; Constantinescu, A. Plastic strain localization induced by microstructural gradient in laser cladding repaired structures. *Theor. Appl. Fract. Mech.* **2020**, *107*, 102520. [CrossRef]
60. Cui, Y.; Shen, J.; Geng, K.; Hu, S. Fabrication of $FeCoCrNiMnAl_{0.5}$-FeCoCrNiMnAl gradient HEA coating by laser cladding technique. *Surf. Coat. Technol.* **2021**, *412*, 127077. [CrossRef]
61. Wang, Q.; Li, Q.; Zhang, L.; Chen, D.X.; Jin, H.; Li, J.D.; Zhang, J.W.; Ban, C.Y. Microstructure and properties of Ni-WC gradient composite coating prepared by laser cladding. *Ceram. Int.* **2022**, *48*, 7905–7917. [CrossRef]
62. Chen, L.; Chen, Y.; Chen, X.; Yu, T.; Wang, Z. Microstructure and properties of in situ TiC/Ni functionally gradient coatings by powder-fed laser cladding. *Ceram. Int.* **2022**, *48*, 36789–36801. [CrossRef]
63. Zhang, S.; Sun, Y.; Cheng, W.; Chen, Y.; Gu, J.; Chen, G. Microstructure and tribological behavior of $CoCrFeNiMo_{0.2}$/SiC high-entropy alloy gradient composite coating prepared by laser cladding. *Surf. Coat. Technol.* **2023**, *467*, 129681. [CrossRef]
64. Hao, X.; Liu, H.; Zhang, X.; Tao, J.; Wang, Y.; Yang, C.; Liu, Y. Microstructure and wear resistance of in-situ $TiN/(Nb, Ti)_5Si_3$ reinforced MoNbTaWTi-based refractory high entropy alloy composite coatings by laser cladding. *Appl. Surf. Sci.* **2023**, *626*, 157240. [CrossRef]
65. Sun, D.; Zhu, L.; Cai, Y.; Yan, Y.; Ge, F.; Shan, M.; Tian, Y.; Han, J.; Jiang, Z. Tribology comparison of laser-cladded CrMnFeCoNi coatings reinforced by three types of ceramic ($TiC/NbC/B_4C$). *Surf. Coat. Technol.* **2022**, *450*, 129013. [CrossRef]

66. Huang, C.; Zhang, Y.; Vilar, R.; Shen, J. Dry sliding wear behavior of laser clad TiVCrAlSi high entropy alloy coatings on Ti–6Al–4V substrate. *Mater. Des.* **2012**, *41*, 338–343. [CrossRef]
67. Wen, X.; Cui, X.; Jin, G.; Zhang, X.; Zhang, Y.; Zhang, D.; Fang, Y. Design and characterization of $FeCrCoAlMn_{0.5}Mo_{0.1}$ high-entropy alloy coating by ultrasonic assisted laser cladding. *J. Alloys Compd.* **2020**, *835*, 155449. [CrossRef]